Assessment of local dynamic subgrid-scale models for stochastic coherent adaptive large eddy simulation

By O. V. Vasilyev†, D. E. Goldstein‡, G. De Stefano¶, D. Bodony, D. You AND L. Shunn

This paper describes progress in the ongoing effort to develop the Stochastic Coherent Adaptive Large Eddy Simulation (SCALES) methodology for modeling of inhomogeneous turbulent flows. The SCALES approach has the potential for significant improvement over regular grid LES methodologies with its ability to resolve and dynamically track the most energetic coherent structures in a turbulent flow through dynamic grid adaptation based on wavelet threshold filtering. Two types of local subgrid scale models were evaluated: Lagrangian path-line/tube dynamic model, based on an extension of the original formulation of Meneveau *et al.* and local one-equation dynamic closure models based on the subgrid scale turbulent kinetic energy. Preliminary numerical experiments are conducted for freely decaying homogeneous turbulence at $Re_\lambda = 72$. Good results are obtained in terms of both grid compression and low-order flow statistics. It has been shown that the SCALES simulations closely match the DNS energy decay with less that 0.5% of the modes of the comparable DNS. The SCALES results were also compared to fully de-aliased LES calculations. The SCALES results outperformed those of the LES at a similar field compression, mainly in the ability to closely match the DNS energy spectra over the full spectral range.

1. Introduction

When dealing with complex turbulent flows, current LES methods rely on, at best, a zonal grid adaptation strategy to attempt to minimize the computational cost. This mesh is typically static and chosen in a somewhat subjective manner to ensure the adequate resolution for different possible flow realizations. While an improvement over the use of regular grids, these methods fail to resolve the high wavenumber components of spatially and temporarily intermittent coherent eddies that typify turbulent flows, thus neglecting valuable physical information. At the same time, the flow is over-resolved in regions between the coherent eddies, consequently wasting computational resources. Finally, as pointed out by Pope (2004), local filter width in most LES implementations is coupled (often proportional) to local mesh size, which makes LES results dependent on the computational grid.

Recently, a novel approach to turbulent complex flow simulation, called Stochastic Coherent Adaptive Large Eddy Simulation (SCALES) has been introduced (Goldstein *et al.* 2004; Goldstein & Vasilyev 2004; Goldstein *et al.* 2005). This method addresses the

† University of Colorado at Boulder, CO
‡ Northwest Research Associates, Inc., CORA Division, CO
¶ Seconda Universitá di Napoli, Italy

above mentioned shortcomings of LES by using a wavelet thresholding filter to dynamically resolve and "track" the most energetic coherent structures during the simulation. The less energetic unresolved modes, the effect of which must be modeled, have been shown to be composed of a minority of coherent modes that dominate the total subgrid scale (SGS) dissipation and a majority of incoherent modes that, due to their decorrelation with the resolved modes, add little to the total SGS dissipation (Goldstein & Vasilyev 2004; De Stefano *et al.* 2005). The physical coherent/incoherent composition of the SGS modes is reflected in the naming of the SCALES methodology, yet as pointed out in Goldstein & Vasilyev (2004) this physical coherent/incoherent composition of the SGS modes is also present in classical LES implementations. For this work, as in much of classical LES research, only the coherent part of the SGS modes will be modeled using a deterministic SGS stress model.

The first step toward the construction of SGS models for SCALES was undertaken during the 2004 CTR Summer Program goldstein-vasilyev-kevlahan:2004, wherein a global dynamic eddy viscosity model based on Germano's classical dynamic procedure redefined in terms of two wavelet thresholding filters was developed. The main drawback of this formulation is the use of a global (spatially non-variable) Smagorinsky model coefficient. The use of a global dynamic model unnecessarily limits the SCALES approach to flows with at least one homogeneous direction. This is unfortunate since the dynamic adaptability of SCALES is ideally suited to fully inhomogeneous flows.

In this paper two different formulations of local dynamic SGS model were explored:

1. Modified Germano's dynamic procedure redefined in terms of wavelet thresholding filters with a modified Lagrangian path-line/tube averaging procedure (Meneveau *et al.* 1996), and
2. SGS kinetic energy based model, where an additional transport equation for the SGS kinetic energy is solved to enforce the energy budget between resolved and unresolved motions.

The rest of the paper is organized as follows. The SCALES methodology for the numerical solution of turbulent flows is briefly reviewed in Section 2. Namely, after defining the wavelet–thresholding filter, the SCALES governing equations are introduced, along with the method for the numerical solution. The local dynamic Smagorinsky model with Lagrangian path-line/tube averaging is discussed in Section 3. The SGS models based on subgrid scale turbulent kinetic energy are described in Section 4. In particular, two different dynamic one–equation SGS models based on eddy viscosity and the "dynamic structure" assumption are proposed. Preliminary results for the numerical simulation of decaying isotropic turbulence are presented in Section 5 and, finally, some concluding remarks are given in Section 6.

2. Stochastic coherent adaptive large eddy simulation

2.1. *Wavelet thresholding filter*

Let us very briefly outline the main features of the wavelet thresholding filter. More details can be found, for instance, in Daubechies (1992). A velocity field $u_i(\mathbf{x})$ can be represented in terms of wavelet basis functions as

$$u_i(\mathbf{x}) = \sum_{\mathbf{l}\in\mathcal{L}^0} c^0_{\mathbf{l}}\phi^0_{\mathbf{l}}(\mathbf{x}) + \sum_{j=0}^{+\infty}\sum_{\mu=1}^{2^n-1}\sum_{\mathbf{k}\in\mathcal{K}^{\mu,j}} d^{\mu,j}_{\mathbf{k}}\psi^{\mu,j}_{\mathbf{k}}(\mathbf{x}), \tag{2.1}$$

where $\phi^0_{\mathbf{k}}(\mathbf{x})$ and $\psi^{\mu,j}_{\mathbf{l}}$ are n-dimensional scaling functions and wavelets of different families and levels of resolution, indexed with μ and j, respectively. One may think of a wavelet decomposition as a multi-level or multi-resolution representation of u_i, where each level of resolution j (except the coarsest one) consists of a family of wavelets $\psi^{\mu,j}_{\mathbf{l}}$ having the same scale but located at different positions. Scaling function coefficients represent the averaged values of the field, while the wavelet coefficients represent the details of the field at different scales.

Wavelet filtering is performed in wavelet space using wavelet coefficient thresholding, which can be considered as a non-linear filter that depends on each flow realization. The wavelet thresholding filter is defined by,

$$\overline{u_i}^{>\epsilon}(\mathbf{x}) = \sum_{\mathbf{l}\in\mathcal{L}^0} c^0_{\mathbf{l}}\phi^0_{\mathbf{l}}(\mathbf{x}) + \sum_{j=0}^{+\infty}\sum_{\mu=1}^{2^n-1} \sum_{\substack{\mathbf{k}\,\in\,\mathcal{K}^{\mu,j} \\ |d^{\mu,j}_{\mathbf{k}}|\,>\,\epsilon U_i}} d^{\mu,j}_{\mathbf{k}}\psi^{\mu,j}_{\mathbf{k}}(\mathbf{x}), \tag{2.2}$$

where $\epsilon > 0$ stands for the non-dimensional (relative) threshold value, U_i being the (absolute) dimensional velocity scale. The latter can be specified in many ways. For instance, in this work we use $U_i = \|\mathbf{u}\|_2$.

The major strength of wavelet filtering is in the ability to compress the solution. For turbulent fields, that contain isolated high-energy structures on a low-energy background, most wavelet coefficients are small. Thus, good approximation can be retained even after discarding a large number of wavelets with small coefficients. From an intuitive point of view, in wavelet decomposition (2.1), the coefficient $d^{\mu,j}_{\mathbf{k}}$ is small unless u_i has significant variation on the level of resolution (scale) j, in the immediate vicinity of wavelet $\psi^{\mu,j}_{\mathbf{k}}(\mathbf{x})$.

2.2. *Wavelet-filtered Navier-Stokes equations*

When applying the wavelet thresholding filter to the Navier-Stokes equations, each variable should be filtered, according to Eq. (2.2), with a corresponding absolute scale. However, this would lead to numerical complications due to the one-to-one correspondence between wavelet locations and grid points. In particular, each variable would be solved on a different numerical grid. In order to avoid this difficulty, the coupled wavelet thresholding strategy is used in the present study. Namely, after constructing the masks of significant wavelet coefficients for each primary variable, the union of these masks results in a global thresholding mask that is used for filtering each term. Note that other additional variables, like vorticity or strain rate, can be used for constructing the global mask.

Once the global mask is constructed, one can view the wavelet thresholding as local low-pass filtering, where the high frequencies are removed according to the global mask. Such an interpretation of wavelet threshold filtering highlights the similarity between SCALES and classical LES approaches. However, the wavelet filter is drastically different from LES filters, primarily because it changes in time following the evolution of the solution, which, in turn, results in an adaptive computational grid that tracks the areas of locally significant energy in physical space.

Therefore, the SCALES equations for incompressible flow, which describe the evolution of the most energetic coherent vortices in the flow field, can be formally obtained by applying the wavelet thresholding filter to the incompressible Navier-Stokes equations:

$$\frac{\partial \overline{u_i}^{>\epsilon}}{\partial x_i} = 0, \tag{2.3}$$

$$\frac{\partial \overline{u_i}^{>\epsilon}}{\partial t} + \frac{\partial (\overline{u_i}^{>\epsilon}\,\overline{u_j}^{>\epsilon})}{\partial x_j} = -\frac{1}{\rho}\frac{\partial \overline{p}^{>\epsilon}}{\partial x_i} + \nu \frac{\partial^2 \overline{u_i}^{>\epsilon}}{\partial x_j \partial x_j} - \frac{\partial \tau_{ij}}{\partial x_j}, \tag{2.4}$$

where ρ, ν are the constant density and kinematic viscosity, and p stands for the pressure. As a result of the filtering process, the unresolved quantities

$$\tau_{ij} = \overline{u_i u_j}^{>\epsilon} - \overline{u_i}^{>\epsilon}\,\overline{u_j}^{>\epsilon}, \tag{2.5}$$

commonly referred to as SGS stresses, are introduced. They represent the effect of unresolved (less energetic) coherent and incoherent eddies on the resolved (energetic) coherent vortices. As usual in a LES approach, in order to close Eqs. (2.4), an SGS model is needed to express the unknown stresses in terms of the resolved field.

2.3. *Numerical implementation*

The SCALES methodology is implemented using the dynamically adaptive wavelet collocation (DAWC) method (e.g., Vasilyev 2003). The DAWC method is ideal for the actual approach as it combines the resolution of the energetic coherent modes in a turbulent flow with the simulation of their temporal evolution. The wavelet collocation method employs wavelet compression as an integral part of the numerical algorithm such that the solution is obtained with the minimum number of grid points for a given accuracy.

Briefly, the DAWC method is an adaptive, variable-order method for solving partial differential equations with localized structures that change their location and scale. As the computational grid automatically adapts to the solution, both in position and scale, one does not have to know *a priori* where the regions of high gradients or localized structures in the flow exist. Also, the method is based on second-generation wavelets (Sweldens 1998), which allow the order of the wavelet (and hence of the numerical method) to be easily varied. The method has a computational complexity $O(N)$, N being the number of wavelets retained in the calculation, i.e., those wavelets with significant coefficients plus nearest neighbors.

3. Lagrangian dynamic SGS model

The primary objective of the current work is to develop a local SGS model for SCALES of inhomogeneous turbulent flows. In previous work a dynamic Smagorinsky model with a global (spatially non-variable) coefficient has been developed and successfully tested for decaying isotropic turbulence (Goldstein *et al.* 2004). In this work this idea is further extended by exploring the use of a local Lagrangian dynamic model (Meneveau *et al.* 1996). Following Goldstein *et al.* (2004), where it was shown that when a wavelet thresholding filter is applied to the velocity field, the resulting SGS stresses scale like ϵ^2, the following Smagorinsky-type eddy-viscosity model is used for simulating the deviatoric part (hereafter noted with a star) of the SGS stress tensor (2.5):

$$\tau^*_{ij} \cong -2C_S \Delta^2 \epsilon^2 \left|\overline{S}^{>\epsilon}\right| \overline{S_{ij}}^{>\epsilon}, \tag{3.1}$$

where $\overline{S_{ij}}^{>\epsilon} = \frac{1}{2}\left(\frac{\partial \overline{u_i}^{>\epsilon}}{\partial x_j} + \frac{\partial \overline{u_j}^{>\epsilon}}{\partial x_i}\right)$ is the resolved rate-of-strain tensor and $\Delta(\mathbf{x}, t)$ is the *local* characteristic vortical lengthscale *dynamically* defined by the wavelet thresholding filter. Note that Δ is distinctively different from the classical LES, where the local filter width is defined *statically*.

Following the modified Germano's dynamic procedure redefined in terms of two wavelet thresholding filters, originally introduced in Goldstein *et al.* (2004), the SGS stress cor-

responding to the wavelet test filter at twice the threshold, noted $\overline{(\cdot)}^{>2\epsilon}$, is defined as

$$T_{ij} = \overline{u_i u_j}^{>2\epsilon} - \overline{u_i}^{>2\epsilon}\,\overline{u_j}^{>2\epsilon}. \tag{3.2}$$

Note that, the wavelet filter being a projection operator, by definition, it holds $\overline{\overline{(\cdot)}^{>\epsilon}}^{>2\epsilon} \equiv \overline{(\cdot)}^{>2\epsilon}$. Filtering Eq. (2.5) at the test filter level and combining with Eq. (3.2) results in the following modified Germano identity for the Leonard stresses:

$$L_{ij} \equiv T_{ij} - \overline{\tau_{ij}}^{>2\epsilon} = \overline{\overline{u_i}^{>\epsilon}\overline{u_j}^{>\epsilon}}^{>2\epsilon} - \overline{u_i}^{>2\epsilon}\,\overline{u_j}^{>2\epsilon}. \tag{3.3}$$

Exploiting the model (3.1) and the analogous relation for the test filtered SGS stresses

$$T^*_{ij} \cong -2C_S\Delta^2\,(2\epsilon)^2\left|\overline{S}^{>2\epsilon}\right|\overline{S_{ij}}^{>2\epsilon}, \tag{3.4}$$

one obtains

$$\overline{2C_S\Delta^2\epsilon^2\left|\overline{S}^{>\epsilon}\right|\overline{S_{ij}}^{>\epsilon}}^{>2\epsilon} - 2C_S\Delta^2\,(2\epsilon)^2\left|\overline{S}^{>2\epsilon}\right|\overline{S_{ij}}^{>2\epsilon} = L^*_{ij}. \tag{3.5}$$

A least square solution to (Eq. 3.5) leads to the following local Smagorinsky model coefficient definition:

$$C_S(\mathbf{x},t)\epsilon^2 = \frac{L^*_{ij}M_{ij}}{M_{nk}M_{nk}}, \tag{3.6}$$

where

$$M_{ij} \equiv 2\Delta^2\left[\overline{\left|\overline{S}^{>\epsilon}\right|\overline{S_{ij}}^{>\epsilon}}^{>2\epsilon} - 4\left|\overline{S}^{>2\epsilon}\right|\overline{S_{ij}}^{>2\epsilon}\right]. \tag{3.7}$$

The coefficient C_S can be actually positive or negative, which allows for local backscatter of energy from unresolved to resolved modes. However, it has been found that negative values of C_S cause numerical instabilities. To avoid this, for homogeneous flow, one can introduce an average over homogeneous directions. This procedure results in a global dynamic model (Goldstein *et al.* 2004).

In this study we follow a Lagrangian dynamic model formulation (Meneveau *et al.* 1996) and take the statistical averages over the trajectory of a fluid particle:

$$\mathcal{I}_{LM}(\boldsymbol{x},t) = \frac{1}{T}\int_{-\infty}^{t} e^{\frac{\tau-t}{T}} L_{ij}(\boldsymbol{x}(\tau),\tau)\,M_{ij}(\boldsymbol{x}(\tau),\tau)\,d\tau, \tag{3.8}$$

$$\mathcal{I}_{MM}(\boldsymbol{x},t) = \frac{1}{T}\int_{-\infty}^{t} e^{\frac{\tau-t}{T}} M_{ij}(\boldsymbol{x}(\tau),\tau)\,M_{ij}(\boldsymbol{x}(\tau),\tau)\,d\tau, \tag{3.9}$$

which leads to the following local Smagorinsky model coefficient:

$$C_S(\mathbf{x},t)\epsilon^2 = \frac{\mathcal{I}_{LM}}{\mathcal{I}_{MM}}. \tag{3.10}$$

To avoid the computationally expensive procedure of Lagrangian path-line averaging, we follow Meneveau *et al.* (1996) and differentiate Eqs. (3.8) and (3.9) with respect to time to obtain the following evolution equations for $\mathcal{I}_{LM}$ and $\mathcal{I}_{MM}$:

$$\frac{\partial\mathcal{I}_{LM}}{\partial t} + \overline{u_l}^{>\epsilon}\frac{\partial\mathcal{I}_{LM}}{\partial x_l} = \frac{1}{T}(L_{ij}M_{ij} - \mathcal{I}_{LM}), \tag{3.11}$$

$$\frac{\partial\mathcal{I}_{MM}}{\partial t} + \overline{u_l}^{>\epsilon}\frac{\partial\mathcal{I}_{MM}}{\partial x_l} = \frac{1}{T}(M_{nk}M_{nk} - \mathcal{I}_{MM}). \tag{3.12}$$

As in Meneveau *et al.* (1996) the relaxation time scale T is defined as $T(\mathbf{x},t) = \theta\Delta\,(\mathcal{I}_{LM}\mathcal{I}_{MM})^{-1/8}$, θ being a dimensionless parameter of order unity.

The equations (3.11) and (3.12) should be solved together with the SCALES equations, (2.3) and (2.4). It should be noticed that both $\mathcal{I}_{LM}$ and $\mathcal{I}_{MM}$ have higher frequency content when compared to the velocity field. This is due to two main factors: the quartic character of nonlinearity of $\mathcal{I}_{LM}$ and $\mathcal{I}_{MM}$ with respect to velocity and the creation of small scales due to chaotic convective mixing. Thus, in order to adequately resolve both $\mathcal{I}_{LM}$ and $\mathcal{I}_{MM}$, one needs to have a substantially finer computational mesh than the one required by the velocity field, which is impractical. To by-pass this problem we consider two different extensions of the Lagrangian path-line averaging: Lagrangian path-tube averaging and Lagrangian path-line diffusive averaging.

The Lagrangian path-tube averaging consist of taking the statistical filtered averages over the trajectory of a fluid particle:

$$\mathcal{I}_{LM}(\boldsymbol{x},t) = \frac{1}{T}\int_{-\infty}^{t}\iiint_{D} e^{\frac{\tau-t}{T}} G(\boldsymbol{y}-\boldsymbol{x}(\tau),\tau)\, L_{ij}(\boldsymbol{x}(\tau),\tau)\, M_{ij}(\boldsymbol{x}(\tau),\tau)\, d\tau d\boldsymbol{y}, \quad (3.13)$$

$$\mathcal{I}_{MM}(\boldsymbol{x},t) = \frac{1}{T}\int_{-\infty}^{t}\iiint_{D} e^{\frac{\tau-t}{T}} G(\boldsymbol{y}-\boldsymbol{x}(\tau),\tau)\, M_{ij}(\boldsymbol{x}(\tau),\tau)\, M_{ij}(\boldsymbol{x}(\tau),\tau)\, d\tau d\boldsymbol{y}, \quad (3.14)$$

where $G(\boldsymbol{x},\tau)$ is the local low-pass filter. Note that the low-pass filter averages the values in the neighborhood of the path-line, effectively making in path-tube averaging. Also note that if $G(\boldsymbol{x},\tau)=1$, i.e., no additional spatial filter is applied, the formulations are identical to the one in (Meneveau *et al.* 1996). This modified averaging procedure leads to the following evolution equations for $\mathcal{I}_{LM}$ and $\mathcal{I}_{MM}$:

$$\frac{\partial \mathcal{I}_{LM}}{\partial t} + \overline{u}_l^{>\epsilon}\frac{\partial \mathcal{I}_{LM}}{\partial x_l} = \frac{1}{T}\left(\overline{L_{ij}M_{ij}}^{\,\mathrm{LP}} - \mathcal{I}_{LM}\right), \quad (3.15)$$

$$\frac{\partial \mathcal{I}_{MM}}{\partial t} + \overline{u}_l^{>\epsilon}\frac{\partial \mathcal{I}_{MM}}{\partial x_l} = \frac{1}{T}\left(\overline{M_{nk}M_{nk}}^{\,\mathrm{LP}} - \mathcal{I}_{MM}\right), \quad (3.16)$$

where $\overline{(\cdot)}^{\,\mathrm{LP}}$ defines low-pass filtering based on $G(\boldsymbol{x},\tau)$.

In the Lagrangian path-line diffusive averaging an additional artificial diffusion term is added to the evolution equations:

$$\frac{\partial \mathcal{I}_{LM}}{\partial t} + \overline{u}_l^{>\epsilon}\frac{\partial \mathcal{I}_{LM}}{\partial x_l} = \frac{1}{T}(L_{ij}M_{ij} - \mathcal{I}_{LM}) + \mathcal{D}_{\mathcal{I}}\frac{\partial^2 \mathcal{I}_{LM}}{\partial x_j \partial x_j}, \quad (3.17)$$

$$\frac{\partial \mathcal{I}_{MM}}{\partial t} + \overline{u}_l^{>\epsilon}\frac{\partial \mathcal{I}_{MM}}{\partial x_l} = \frac{1}{T}(M_{nk}M_{nk} - \mathcal{I}_{MM}) + \mathcal{D}_{\mathcal{I}}\frac{\partial^2 \mathcal{I}_{MM}}{\partial x_j \partial x_j}. \quad (3.18)$$

To avoid the creation of small scales, the diffusion time scale, $\Delta^2/\mathcal{D}_{\mathcal{I}}$, should be smaller than the convective time scale associated with local strain, $\left|\overline{S}^{>\epsilon}\right|^{-1}$, which results in $\mathcal{D}_{\mathcal{I}} = C_{\mathcal{I}}\Delta_\epsilon^2\left|\overline{S}^{>\epsilon}\right|$, where C_I is a dimensionless parameter of order unity.

Combining these two approaches results in the Lagrangian path-line/tube averaged equations:

$$\frac{\partial \mathcal{I}_{LM}}{\partial t} + \overline{u}_l^{>\epsilon}\frac{\partial \mathcal{I}_{LM}}{\partial x_l} = \frac{1}{T}\left(\overline{L_{ij}M_{ij}}^{\,\mathrm{LP}} - \mathcal{I}_{LM}\right) + \mathcal{D}_{\mathcal{I}}\frac{\partial^2 \mathcal{I}_{LM}}{\partial x_j \partial x_j}, \quad (3.19)$$

$$\frac{\partial \mathcal{I}_{MM}}{\partial t} + \overline{u}_l^{>\epsilon}\frac{\partial \mathcal{I}_{MM}}{\partial x_l} = \frac{1}{T}\left(\overline{M_{nk}M_{nk}}^{\,\mathrm{LP}} - \mathcal{I}_{MM}\right) + \mathcal{D}_{\mathcal{I}}\frac{\partial^2 \mathcal{I}_{MM}}{\partial x_j \partial x_j}. \quad (3.20)$$

Note that the case $G = 1$ and $C_{\mathcal{I}} = 0$ is equivalent to the original Lagrangian formulation of Meneveau *et al.* (1996).

4. Kinetic energy based model

An alternative mechanism to achieve locality of the SGS model is to solve an additional transport equation for the subgrid scale kinetic energy, $k_{\rm sgs}$. This explicitly enforces the energy budget between resolved and unresolved motions, while providing a local feedback mechanism that automatically stabilizes the solution without performing any averaging procedure and allowing for local energy backscatter. Following Ghosal *et al.* (1995) the transport equation for the SGS kinetic energy can be written as

$$\frac{\partial k_{\rm sgs}}{\partial t} + \overline{u}_j^{>\epsilon} \frac{\partial k_{\rm sgs}}{\partial x_j} = \Pi - \epsilon_{\rm sgs} + \nu \frac{\partial^2 k_{\rm sgs}}{\partial x_j \partial x_j} + \frac{\partial}{\partial x_j} \left(\nu_t \frac{\partial k_{\rm sgs}}{\partial x_j} \right), \tag{4.1}$$

where

$$k_{\rm sgs} = \frac{1}{2} \left(\overline{u_i u_i}^{>\epsilon} - \overline{u_i}^{>\epsilon} \overline{u_i}^{>\epsilon} \right), \tag{4.2}$$

ν_t is local turbulent eddy viscosity, and Π and $\epsilon_{\rm sgs}$ stand for the SGS kinetic energy production and dissipation, respectively.

The SGS energy production due to the interaction between resolved and unresolved motions, that is $\Pi = -\tau_{ij} \overline{S}_{ij}^{>\epsilon}$, takes a fundamental role in modeling procedures based on $k_{\rm sgs}$, as it provides a local feedback mechanism that stabilizes the simulation. If there is energy backscatter from unresolved to resolved motions, the SGS kinetic energy locally decreases but, according to Eq. (4.4), the SGS stresses decrease as well, suppressing the reverse flow of energy. The SGS energy dissipation rate, using simple scaling arguments, can be modeled as $\epsilon_{\rm sgs} \cong C_\epsilon \frac{k_{\rm sgs}^{3/2}}{\Delta}$, C_ϵ being a dimensionless model coefficient (e.g., see Schumann 1975; Ghosal *et al.* 1995). In principle, C_ϵ could be determined by means of a dynamic procedure (e.g., , Kim & Menon 1999). However, in order to access the general applicability of the model, $C_\epsilon = 1$ is simply prescribed in this work.

The wavelet-filtered Navier-Stokes equations (2.4) and the SGS kinetic energy transport equation (4.1) can be simultaneously solved, provided that the subgrid scale stress, τ_{ij}, is modeled as a function of resolved velocity and SGS kinetic energy. In this paper we have considered both eddy-viscosity and non-eddy viscosity types of models. These models are discussed next.

4.1. *Localized eddy-viscosity model*

Following Ghosal *et al.* (1995) the turbulent eddy viscosity is defined as

$$\nu_t = C_\nu \Delta k_{\rm sgs}^{1/2}, \tag{4.3}$$

C_ν being a dimensionless coefficient and $\Delta(\mathbf{x}, t)$ the local characteristic lengthscale dynamically defined by the wavelet thresholding filter. This way, Eq. (3.1) becomes

$$\tau_{ij}^* \cong -2 C_\nu \Delta k_{\rm sgs}^{1/2} \overline{S}_{ij}^{>\epsilon}. \tag{4.4}$$

To complete the SGS modeling procedure, the evolution of $k_{\rm sgs}$ is modeled by Eq. (4.1). By exploiting the model (4.4), the wavelet-filtered Navier-Stokes equations (2.4) and the SGS kinetic energy equation (4.1) constitute a closed system of coupled equations that is solved with the DAWC methodology briefly described in Section 2.3. In particular, the global thresholding mask for wavelet filtering is constructed by also considering the SGS kinetic energy field.

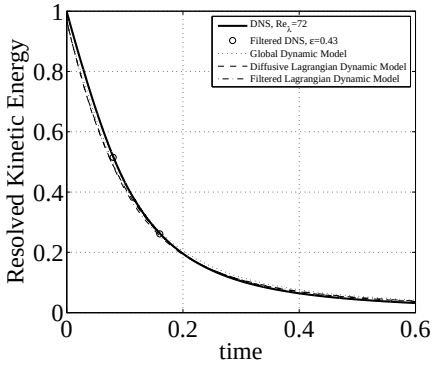

FIGURE 1. Energy decay for SCALES with Lagrangian path-line diffusive averaging model (– – – –), filtered Lagrangian path-tube averaging model (–·–·–), global dynamic Smagorinsky model (·····), and for comparison DNS (———). Wavelet filtered DNS is shown for 2 stations at which energy spectra will be presented below(∘).

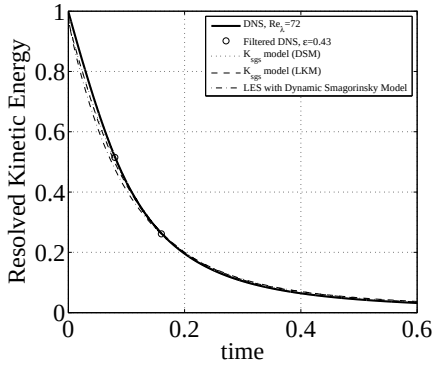

FIGURE 2. Energy decay for SCALES with dynamic structure model (·····), localized eddy-viscosity model (– – – –), LES with global dynamic Smagorinsky model (–·–·–), and for comparison DNS (———). Wavelet filtered DNS is shown for 2 stations at which energy spectra will be presented below(∘).

The above one-equation model will be referred to as localized kinetic energy based model (for discussion, LKM) in the following. It is worth stressing that, though the model coefficient is *a priori* prescribed, nevertheless the LKM procedure is in someway dynamic as it takes into account the local energy transfer between resolved and unresolved motions for the ongoing simulation. For the numerical experiments carried out in this work, the value $C_\nu = 0.06$ is prescribed for the LKM coefficient. The fully dynamic procedure is a subject of future work.

4.2. *Dynamic structure model*

Following Pomraning & Rutland (2002), the "dynamic structure" model (hereafter referred to as DSM) exploits the significant similarity between the SGS and the Leonard stresses that has been observed in real as well as numerical experiments (e.g., Liu *et al.* 1994). Due to the existing similarity between the SGS and the Leonard stresses, one can assume $\tau_{ij}/\tau_{ll} \cong L_{ij}/L_{hh}$, which results in the following definition for the SGS stresses (Pomraning & Rutland 2002; Chumakov & Rutland 2005):

$$\tau_{ij} \cong \frac{2k_{\rm sgs}}{L_{hh}} L_{ij}. \tag{4.5}$$

It is important to note that in order to ensure the positiveness of the trace of the Leonard stress tensor, L_{hh}, we no longer can utilize the wavelet thresholding filter with twice the threshold as in Eq. (3.3). Instead, a local positive low-pass filter with the filter width twice the local characteristic lengthscale $\Delta(\mathbf{x}, t)$ is used.

Analogously to the LKM procedure, the model involves an additional transport equation for the SGS kinetic energy, $k_{\rm sgs}$. Due to the non-eddy viscosity nature of the dynamic structure model, the transport equation (4.1) can no longer be used. Instead the following equation for SGS kinetic energy evolution is solved

$$\frac{\partial k_{\rm sgs}}{\partial t} + \overline{u}_j^{>\epsilon} \frac{\partial k_{\rm sgs}}{\partial x_j} = \Pi - \epsilon_{\rm sgs} + \nu \frac{\partial^2 k_{\rm sgs}}{\partial x_j \partial x_j}, \tag{4.6}$$

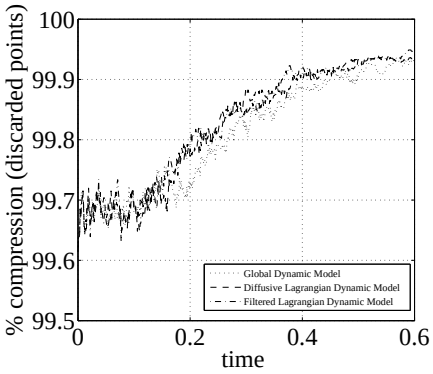

FIGURE 3. Field compression for SCALES with Lagrangian path-line diffusive averaging model (– – – –), filtered Lagrangian path-tube averaging model (–·–·– –), and global dynamic Smagorinsky model (·····).

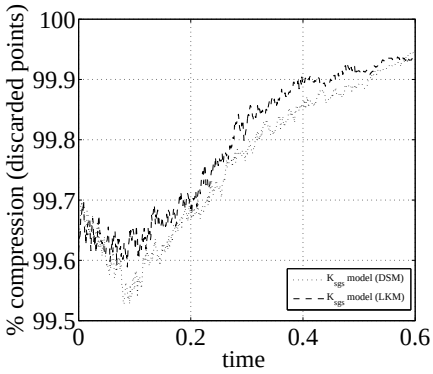

FIGURE 4. Field compression for SCALES with dynamic structure model (·····), localized eddy-viscosity model (– – – –). For comparison, the compression for LES with global dynamic Smagorinsky model was 98.4%.

where, differently from the general equation (4.1), the SGS energy diffusion due to turbulent viscosity is not present. With the adopted SGS stress definition, the SGS kinetic energy production becomes

$$\Pi = -\frac{2k_{\rm sgs}}{L_{hh}} L_{ij} \overline{S}_{ij}^{>\epsilon}, \tag{4.7}$$

and can show both signs, thus allowing for local energy backscatter. This way, the model (4.5) overcomes some difficulties, if not mathematical inconsistencies, associated to the classical dynamic Smagorinsky modeling approach. Furthermore, Eq. (4.5) does not involve the definition of any model coefficient.

Note the transparent similarity of the DSM and scale similarity Bardina models (Bardina *et al.* 1983). However, due to non-linear rescaling of the Leonard stress in the DSM approach, these two models are not identical. Furthermore, as pointed out by Pomraning & Rutland (2002) and confirmed in this study, the DSM does not show the insufficient energy dissipation characteristic of the Bardina model (e.g., see Kim & Menon 1999).

5. Results

In this paper, the preliminary results of SCALES simulations with Lagrangian path-line/tube averaging and SGS kinetic energy models applied to incompressible isotropic decaying turbulence are presented. The initial velocity field is a realization of a statistically stationary turbulent flow at $Re_\lambda = 72$, as provided by a pseudo-spectral DNS database (De Stefano *et al.* 2005). In all SCALES cases shown the wavelet thresholding parameter is set to $\epsilon = 0.43$, as previously discussed.

The Lagrangian path-line/tube modeling variables are initialized as $\mathcal{I}_{MM} = M_{nk}M_{nk}$ and $\mathcal{I}_{LM} = \bar{C}_s\epsilon^2\mathcal{I}_{MM}$, $\bar{C}_s$ being the volume averaged value. For the time relaxation scale definition, the value $\theta = 0.75$ is chosen. The diffusion coefficient $C_{\mathcal{I}} = 5$ is used for the local dynamic model with Lagrangian path-line diffusive averaging, while for the Lagrangian path-tube averaging model $C_{\mathcal{I}}$ is set to zero. Both DSM and LKM models are initialized as

$$k_{\rm sgs} = \alpha \frac{L_{ii}}{\langle L_{ii} \rangle} \frac{\langle \overline{u_i}^{>\epsilon} \overline{u_i}^{>\epsilon} \rangle}{2}, \tag{5.1}$$

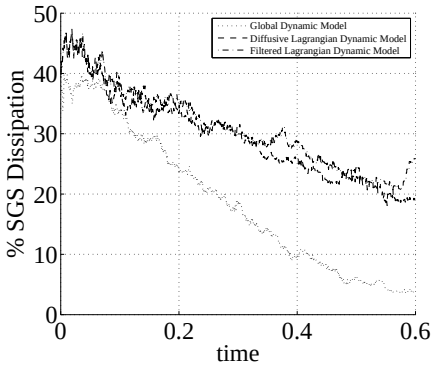

FIGURE 5. Percentage of SGS (modeled) dissipation for SCALES with Lagrangian path-line diffusive averaging model (– – – –), filtered Lagrangian path-tube averaging model (–·–·–), and global dynamic Smagorinsky model (·····).

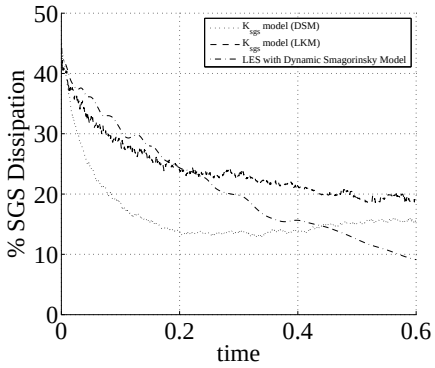

FIGURE 6. Percentage of SGS (modeled) dissipation for SCALES with dynamic structure model (·····), localized eddy-viscosity model (– – – –), and LES with global dynamic Smagorinsky model (–·–·–).

where $\alpha = 0.1$ is the fraction of the resolved turbulent kinetic energy.

In Figs. 1–6 the resolved turbulent kinetic energy decay, grid compression, and percentage of modeled SGS dissipation for SCALES with the Lagrangian path-line/tube averaging and SGS kinetic energy models are compared to SCALES with a global dynamic model (Goldstein *et al.* 2005) (for discussion: GDM) and LES with global dynamic Smagorinsky model. The LES simulation is performed using the non-adaptive wavelet collocation solver on a regular 64^3 grid with the classical dynamic Smagorinsky model. The simulation is de-aliased by performing a wavelet transform on the velocity field and zeroing the highest level wavelet coefficients, thus resulting in a 32^3 solution at the end of the time step. The results of a fully de-aliased pseudo-spectral DNS simulation are shown for reference. The energy shown is normalized with respect to the initial DNS content. The compression stated is always with respect to the maximum field resolution, which in this case is 256^3. Figures 7—10 show the power density spectra at $t = 0.08$ and $t = 0.16$, which are marked in Figs. 1 and 2. The energy spectra of the wavelet filtered DNS is shown with circles.

From these results we can see that the SCALES with Lagrangian path-line/tube averaging and SGS kinetic energy models match closely to the DNS results not only in terms of temporal evolution of the total resolved turbulent kinetic energy but, more importantly, in terms of recovering the DNS spectra over the full spectral range. It is important to emphasize that this close match is achieved using less than 0.5% of the total non-adaptive nodes required for a DNS with the same wavelet solver. Note that while the pseudo-spectral DNS database was run with a resolution of 128^3, the non-adaptive wavelet collocation solver would require twice the resolution (256^3) to compensate for the decreased accuracy associated with the polynomial (finite difference) nature of the wavelet approximation. To highlight the significance of such a close match, it is interesting to compare these results with the results of LES with the global dynamic Smagorinsky model: despite the fact that LES uses more modes (1.56%), it fails to capture the small-scale feature of the spectrum, as well as the total resolved kinetic energy is noticeably below the DNS curve.

It is important to emphasize the unique feature of SCALES approach, namely the

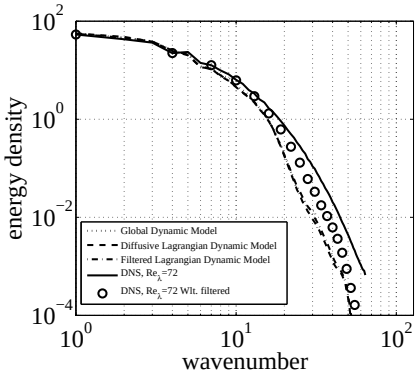

FIGURE 7. Energy density spectra at $t = 0.08$ for DNS (———), filtered DNS (○), SCALES with Lagrangian path-line diffusive averaging model (– – – –), filtered Lagrangian path-tube averaging model (–·–·–), and global dynamic Smagorinsky model (·····).

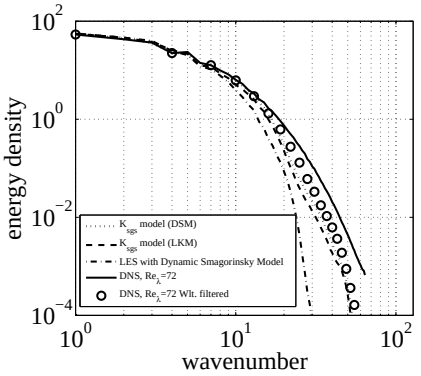

FIGURE 8. Energy density spectra at $t = 0.08$ for DNS (———), filtered DNS (○), SCALES with dynamic structure model (·····), localized eddy-viscosity model (– – – –), and LES with global dynamic Smagorinsky model (–·–·–).

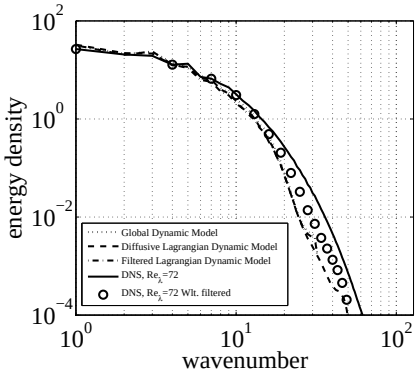

FIGURE 9. Energy density spectra at $t = 0.16$ for DNS (———), filtered DNS (○), SCALES with Lagrangian path-line diffusive averaging model (– – – –), filtered Lagrangian path-tube averaging model (–·–·–), and global dynamic Smagorinsky model (·····).

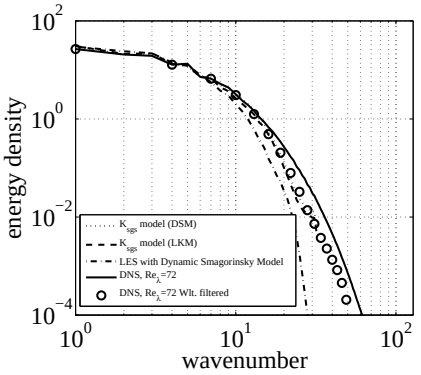

FIGURE 10. Energy density spectra at $t = 0.16$ for DNS (———), filtered DNS (○), SCALES with dynamic structure model (·····), localized eddy-viscosity model (– – – –), and LES with global dynamic Smagorinsky model (–·–·–).

direct coupling of modeled SGS dissipation and grid compression: more points are used for models with lower levels of SGS dissipation. In other words, the SCALES approach has an ability to compensate for the inadequate level of SGS dissipation by adjusting the local resolution and, subsequently, the level of resolved viscous dissipation. Another important aspect that needs to be mentioned is the sensitivity of the SGS kinetic energy models to the initial level of k_{sgs}. Due to the transient nature of the decaying homogeneous turbulence, setting SGS kinetic energy to high results in excessive SGS dissipation, which ultimately leads to wrong energy decay. We believe that situation can be improved by considering a fully dynamic formulation. Finally, the local dynamic Smagorinsky model with Lagrangian diffusive path-line averaging and Lagrangian path-tube averaging show virtually identical results, which highlights the similarities of both averaging approaches.

6. Conclusions

The development of local SGS models is unavoidable for the application of the SCALES methodology to practical engineering problems. In this work, new local SCALES models based on Lagrangian path-line/tube averaging and the subgrid-scale turbulent kinetic energy are developed and assessed in terms of accuracy and efficiency. The results in this work show that local SGS models can be used with the SCALES approach. Further studies for higher Reynolds number flows and the presence of solid walls are currently underway and will be reported in a future publication.

REFERENCES

Bardina, J., Ferziger, J. H. & Reynolds, W. C. 1983 Improved turbulence models based on large eddy simulation of homogeneous incompressible turbulence. *Report TF-19*, Thermosciences Div., Dept. of Mech. Eng., Stanford University.

Chumakov, S. G. & Rutland, C. J. 2005 Dynamic structure subgrid-scale models for large eddy simulation. *Int. J. Numer. Meth. Fluids* **47**, 911–923.

Daubechies, I. 1992 *Ten Lectures on Wavelets. CBMS-NSF Series in Applied Mathematics* 61. Philadelphia: SIAM.

De Stefano, G., Goldstein, D. E. & Vasilyev, O. V. 2005 On the role of sub-grid scale coherent modes in large eddy simulation. *J. Fluid Mech.* **525**, 263–274.

Ghosal, S., Lund, T. S., Moin, P. & Akselvoll, K. 1995 A dynamic localization model for large-eddy simulation of turbulent flows. *J. Fluid Mech.* **286**, 229–255.

Goldstein, D., Vasilyev, O. & Kevlahan, N.-R. 2005 CVS and SCALES simulation of 3D isotropic turbulences. *J. Turbulence* **6** (37), 1–20.

Goldstein, D. E. & Vasilyev, O. V. 2004 Stochastic coherent adaptive large eddy simulation method. *Phys. Fluids* **16**, 2497–2513.

Goldstein, D. E., Vasilyev, O. V. & Kevlahan, N. K.-R. 2004 Adaptive LES of 3D decaying isotropic turbulence. In *Proceedings of the 2004 Summer Program*, Center for Turbulence Research, NASA-Ames/Stanford Univ.

Kim, W.-W. & Menon, S. 1999 An unsteady incompressible navier-stokes solver for large eddy simulation of turbulent flows. *Int. J. Numer. Meth. Fluids* **31**, 983–1017.

Liu, S., Meneveau, C. & Katz, J. 1994 On the properties of similarity subgrid-scale models as deduced from measurements in a turbulent jet. *J. Fluid Mech.* **275**, 83–119.

Meneveau, C., Lund, T. S. & Cabot, W. H. 1996 A Lagrangian dynamic subgrid-scale model of turbulence. *J. Fluid Mech.* **319**, 353–385.

Pomraning, E. & Rutland, C. J. 2002 Dynamic one-equation nonviscosity large-eddy simulation model. *AIAA J.* **40**, 689–701.

Pope, S. B. 2004 Ten questions concerning the large-eddy simulation of turbulent flows. *New J. Phys* **6** (35).

Schumann, U. 1975 Subgrid scale model for finite difference simualtions of turbulent flows in plane channels and annuli. *J. Comp. Phys.* **18**, 376–404.

Sweldens, W. 1998 The lifting scheme: A construction of second generation wavelets. *SIAM J. Math. Anal.* **29**, 511–546.

Vasilyev, O. V. 2003 Solving multi-dimensional evolution problems with localized structures using second generation wavelets. *Int. J. Comp. Fluid Dyn.,* Special issue on High-resolution methods in Computational Fluid Dynamics **17**, 151–168.